Quantitative Determination of Nonradiative Host-to-Activator Energy Transfer Efficiencies in $YBO_3:Eu^{3+}$ and $Y_2O_3:Eu^{3+}$ under Vacuum Ultraviolet Excitation

Tracy Watrous-Kelley and Anthony L. Diaz*

Department of Chemistry, Central Washington University, 400 East University Way, Ellensburg, Washington 98926

Tuan A. Dang

Osram Sylvania, Hawes Street, Towanda, Pennsylvania 18848

Received February 15, 2006

We report on the spectroscopic determination of nonradiative host to activator transfer efficiencies in Eu^{3+}-doped Y_2O_3 and YBO_3 under vacuum ultraviolet excitation. The calculation of transfer efficiency is described, and the transfer efficiency behavior of both hosts is assessed in terms of accepted energy flow models. From our measurements we have concluded that electron−hole pair mobility is greater in Y_2O_3 than in YBO_3 and that the primary reason for the relatively low efficiency of $Y_2O_3:Eu^{3+}$ under 147 nm excitation is loss of excitation energy to surface states. Measurements on the Tm^{3+}-doped hosts indicate that these properties are features of the host rather than of the dopant.

Introduction

Developing a detailed understanding of electron transport processes in solids is important to a wide variety of fields within materials science, including the study of cathode ray phosphors, scintillators, two-photon phosphors, and transparent conducting oxides. Of particular interest to this work are processes associated with vacuum ultraviolet (VUV) excitation of doped solid-state luminescent materials, such as are found in plasma display panels (PDP) and Xe-based mercury-free lamps. The Xe discharge generates excitation photons at 147 and 172 nm, energies that are greater than the electronic band gap of most oxides. Thus, absorption of VUV radiation leads to the creation of an electron−hole (e−h) pair in the host. For luminescence to occur this absorbed energy must be transferred to the activator (dopant). The focus of much of the published research in this area has been primarily on measuring the overall VUV efficiencies of materials of known technological interest. Thus, little is known about the fundamental structure/property relationships that govern host-to-activator energy transfer. In fact, there are few studies that address energy transfer directly, and to our knowledge quantitative transfer efficiency measurements under VUV excitation have not been reported for any material. Maximum theoretical energy efficiencies for VUV excitation are fairly low, and the long-term development of more energy efficient technologies requires a more detailed understanding of the various processes at work in a solid during excitation by VUV radiation. In addition, more refined structure/function models are needed to aid in the discovery of new materials for these applications.

We are undertaking a detailed study of host-to-activator energy transfer under VUV excitation, with the overall goal of developing general relationships between the electronic and crystal structure of a host and the observed host-to-activator transfer efficiency. In this manuscript we report the results of transfer efficiency measurements on $YBO_3:Eu^{3+}$ and $Y_2O_3:Eu^{3+}$. $YBO_3:Eu^{3+}$ is an efficient VUV red phosphor; the Gd co-doped material is already used in PDPs.[1] $Y_2O_3:Eu^{3+}$ is not as bright under VUV excitation and so is not used in PDPs even though the emission color is preferred. In what follows, we show that the difference in VUV efficiencies between these materials can be directly attributed to differences in their transfer efficiency properties. The spectroscopic determination of transfer efficiency is described, and the results are discussed in terms of accepted energy flow models.

Experimental

$YBO_3:Eu^{3+}$ samples were prepared by dissolving stoichiometric ratios of H_3BO_3, Y_2O_3, and Eu_2O_3 in concentrated nitric acid, evaporating the solution to dryness, and firing the dried, ground precipitate in air at 900 °C for 18 h. $Y_2O_3:Eu^{3+}$ samples were prepared using the same procedure without H_3BO_3. Fired compounds were sifted through 40-μm mesh. All materials were found to be crystalline and single phase by powder X-ray diffraction.

Excitation spectra were obtained using a deuterium lamp attached to a VUV monochromator (Acton Research Corp. VM 502) for excitation and an ARC SP-150 UV/vis monochromator with a photomultiplier tube (PMT) for measuring sample emission. Powder samples mount vertically in the chamber at 60° in, 30° out. The lamp, excitation monochromator, and sample chamber are evacuated

* To whom correspondence should be addressed. Phone: 509-963-2818. Fax: 509-963-1050. E-mail: diaza@cwu.edu.

(1) Kim, C.-H.; Kwon, I.-E.; Park, C.-H.; Hwang, Y.-J.; Bae, H.-S.; Yu, B.-Y.; Pyun, C.-H.; Hong, G.-Y. *J. Alloys Compd.* **2000**, *311*, 33.

10.1021/cm060383l CCC: $33.50
Published on Web 05/20/2006

using a diaphragm/turbomolecular pumping station (Pfeiffer Vacuum, TSU 071E), to a base pressure of about 3.0×10^{-5} mbar. Emission spectra are corrected using a NIST calibrated lamp, while excitation spectra are corrected using a sodium salicylate standard.

A second PMT with a sodium salicylate coated window is mounted directly to the sample chamber for collecting reflectance spectra between 115 and 300 nm. This measurement is more challenging on doped samples because the incident radiation generates emission from the sample that is detected along with any reflected light. Thus, three measurements are made. The first is a reflectance measurement with a 377 nm blocking filter between the sample and the detector. This setup collects only the sample emission that results from absorption of incident radiation. The second measurement is done with the blocking filter removed and, therefore, contains both reflectance and emission information. The reflectance spectrum of the sample is determined by taking the difference between these two measurements. A third measurement is done using a MgF_2 standard to correct for lamp and monochromator variation. Throughout these measurements, we found that about 1.5% of reflected light in the VUV reaches the detector with the blocking filter in place (largely because of the geometry of the sample chamber). Although it has only a minimal effect on the results of our analysis, we have included this additional correction in all of our reflectance spectra.

Scanning electron microscope images were obtained using a VEGA TS 5136MM at 20 kV. Depth profiling was obtained using a Leybold INA-3 sputtered neutral mass spectrometer (SNMS). In this device, argon ions were produced by an inductively coupled radio frequency discharge. Ions were extracted from this argon plasma to the sample surface by applying a high-frequency square wave (HFSW) voltage to the target. For these powders, the HFSW conditions were set at 600 V, 400 kHz, and 40% duty cycle. The negative phase of the square wave (40% of cycle duration) enabled the positive ion bombardment of the surface. The positive phase attracted electrons from the plasma to the sample surface, providing optimum charge neutralization. Sputtered neutrals were post-ionized in the plasma and subsequently analyzed by a quadrupole mass spectrometer. A sputtering rate of 0.7 Å/s (vs Ta_2O_5) was obtained under this condition. The profiles displayed were corrected for isotopic ratios only and normalized to 100%. Other sensitivity factors were not accounted for.

Results

Modeling Nonradiative Energy Transfer. Robbins and Dean have outlined in some detail the mechanisms by which activators can trap e−h pairs in solids.[2] The most accepted description of nonradiative energy transfer is a sequential trapping scheme, wherein the electron is trapped at the activator impurity and the hole is subsequently captured. In some systems, hole trapping occurs first. A quantitative evaluation of nonradiative energy transfer must begin with a description of the flow of energy in the host/activator system once an e−h pair is created.

Several such models have been published for cathode ray,[3] scintillator,[4] two-photon[5] and VUV phosphors,[6] and provide the basis for the discussion that follows. When an e−h pair is created in the host it will be captured either by activators or by a variety of killers (impurities or defects). In the context of this discussion, the term killer refers to any trapping mechanism that leads the absorbed energy away from the activator.

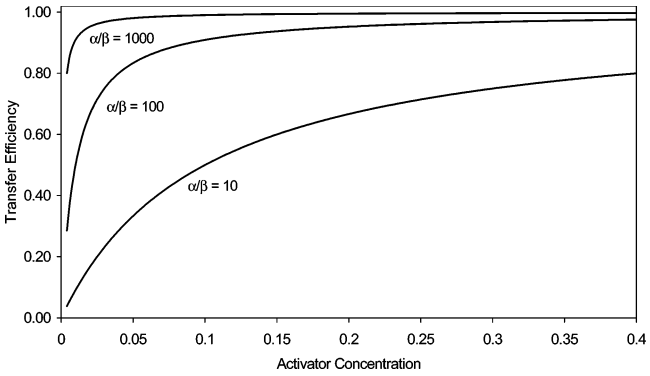

Figure 1. Plots of transfer efficiency, η_t, versus activator concentration for various values of α/β, as calculated from eq 1.

The rate of transfer to killers is a function of several factors, including the killer concentration, the capture cross section of the various killers, and the intrinsic diffusion length, which we call l_0, of an e−h pair in the given solid. The rate of transfer to activators will depend on the activator concentration, the capture cross section of the activator in a given host, and l_0. These rates will also include higher order effects at high excitation densities. Under continuous excitation at low excitation densities, however, these effects can be neglected.[6] For excitation near the band edge of the host, then, energy flow is initially described by a simple first-order competition model,[3,6,7] where the transfer efficiency is given by

$$\eta_t = \frac{\alpha N}{\alpha N + \beta} \tag{1}$$

Here, αN is the rate of transfer to activators (rate constant $\times$ concentration). The killer concentration in a given material is unknown, so β is the overall rate of transfer to bulk killers. If concentrations are given as number densities, then α has units of s^{-1} and β has units of $cm^{-3}s^{-1}$.

Before discussing our experimental results, it is instructive to consider how the α/β ratio affects η_t. Plots of η_t versus activator concentration using eq 1 are shown in Figure 1 for several different α/β ratios. Generally number densities (cm^{-3}) are used to express concentrations, but for purposes of clarity atom % is used here. For each curve, η_t increases with activator concentration, as more ions become available for e−h capture. As the ratio of α/β increases the curves approach 100% efficiency rapidly. At very high α/β, the transfer efficiency is essentially 100% everywhere except at very low concentrations. It is important to note that α/β is a rate constant over a rate. The ratio of capture rates to activator and killers is given by $\alpha N/\beta$. Hidden in this model is the assumption that the intrinsic diffusion length of e−h pairs in the solid is large relative to the distribution of activators. Thus, at low concentrations in some systems there

(2) Robbins, D. J.; Dean, P. *J. Adv. Phys.* **1978**, *27*, 499.
(3) de Leeuw, D. M.; 't Hooft, G. W. *J. Lumin.* **1983**, *28*, 275.
(4) Bartram, R. H.; Lempicki, A. *J. Lumin.* **1996**, *68*, 225.
(5) Kirm, M.; Feldbach, E.; Lushchik, A.; Lushchik, C.; Maaroos, A.; Savikhina, T. *SPIE Proc.* **1997**, *2967*, 18.
(6) Mishra, K. C.; Raukas, M. *J. Electrochem. Soc.* **2004**, *151*, H105.
(7) Klassen, D. B. M.; Mulder, H.; Ronda, C. R. *Phys. Rev. B* **1989**, *39*, 42.

may be a diffusion-limited regime for which eq 1 may overestimate the expected transfer efficiency. This is an important point that will be discussed again later.

The loss of energy to surface states is an extremely important aspect of the study of these processes. The termination of the bulk lattice generally leads to the formation of unique states that act as energy traps under host lattice excitation.[8] The absorption coefficient of the host increases as the incident photon energy is increased beyond the band edge, meaning that a larger fraction of the absorbed energy is distributed at the surface. Thus, there is a greater probability of losing energy to radiationless recombination at surface states as the energy of excitation is increased. Mishra and Raukas have shown that surface loss processes appears as a multiplier to eq 1: $\eta_t = \alpha N/(\alpha N + \beta)\alpha_{be}\tau_h S_{loss}$.[6] Here, $\alpha_{be}\tau_h$ describes the efficiency with which energy absorbed by the host is transferred to the band edge, while S_{loss} is a function of several factors (primarily diffusion length). The term $\alpha_{be}\tau_h S_{loss} = 1$ when there are no surface losses and will decrease toward a value of zero as surface losses increase. Thus, deviations of experimental data from the curves of Figure 1 are an indication of surface loss effects. As the energy of excitation is increased, these effects should become more dominant. In this way, it should be possible to distinguish bulk killer effects from migration to surface states.

Spectroscopic Determination of η_t. In general, the efficiency of host-to-activator energy transfer in a doped phosphor can be estimated by comparing the luminescence efficiency under host excitation to the quantum efficiency of the activator under direct excitation. That is, we can write $\eta_{host} = \eta_t\eta_{act}$ or, alternatively, $\eta_t = \eta_{host}/\eta_{act}$, where η_t is the transfer efficiency, η_{act} is the quantum efficiency of the activator, and η_{host} is the efficiency under host lattice excitation. A transfer efficiency of unity is observed when the efficiency of the material is the same under host or direct excitation, that is, when there are no additional energy loss processes in the host prior to capture of the electron hole pair by the activator. Using this rationale, Lempicki et al. calculated transfer efficiencies in a variety of scintillator materials by comparing light yields under gamma irradiation to known activator quantum efficiencies,[9] while Klassen et al. applied similar reasoning to estimate transfer efficiencies of several oxisulfides under cathode ray excitation.[7] VUV excitation is fundamentally different from those processes in that cathode ray and gamma ray excitation produce many e−h pairs for one absorption event, while absorption of a VUV photon generates a single e−h pair. Thus, VUV excitation is more sensitive to some factors, most particularly the band structure of the host, as will be discussed later.

Our approach to calculating the transfer efficiency begins with a consideration of the individual terms that comprise the total quantum efficiency of a material under VUV excitation. For an absorbed VUV photon flux, Φ_{abs}^{VUV}, the overall quantum efficiency of the phosphor, η_{VUV}, is given by

$$\eta_{VUV} = \frac{\Phi_{em}^{VUV}}{\Phi_{abs}^{VUV}} \tag{2}$$

Here, Φ_{em}^{VUV} is the total emitted photon flux of the material under VUV excitation. This VUV quantum efficiency can be broken down into terms representing the steps involved in the luminescence process:

$$\eta_{VUV} = \eta_t\eta_{act} \tag{3}$$

Substituting the efficiencies in eq 3 with the appropriate photon fluxes yields

$$\frac{\Phi_{em}^{VUV}}{\Phi_{abs}^{VUV}} = \eta_t\frac{\Phi_{em}^{UV}}{\Phi_{abs}^{UV}} \tag{4}$$

Here, "VUV" refers to excitation energies greater than the band gap of the host, while "UV" refers to lower energy photons that directly excite the activator. Solving this equation for the transfer efficiency and rearranging gives

$$\eta_t = \frac{\Phi_{em}^{VUV}}{\Phi_{em}^{UV}}\frac{\Phi_{abs}^{UV}}{\Phi_{abs}^{VUV}} \tag{5}$$

This expression holds when the flux in each ratio is normalized to the same incident photon flux and excitation densities are kept below the saturation limit. Qualitatively, eq 5 can be interpreted in a fairly straightforward manner. A relatively more intense emission under VUV excitation implies a greater transfer efficiency, while relatively smaller VUV absorption indicates a greater VUV quantum efficiency.

A considerable advantage of this technique is that because ratios are used, corrections are canceled out (that is, absolute data are not required). However, some assumptions and shortcomings in the application of this method need to be pointed out. The first is that diffuse reflectance data from powders are being used to represent absorption. Therefore, we are not measuring the absolute absorbance but only the reflectance relative to a standard. Because we are taking a ratio to calculate transfer efficiency, the calculation breaks down only if there is a difference in the angular dependence of the reflected intensity between the VUV and the UV wavelengths. Therefore, we have assumed that if any such difference exists it is not significant over the range under study.

The second point relates to our estimate of the emitted photon fluxes under UV and VUV excitation. In our calculations, we have taken these ratios directly from the excitation spectra of the $^5D_0 \rightarrow {}^7F_2$ transition of Eu^{3+} (612 nm) in each compound. Our motivation for using the excitation spectra comes from the fact that if integrated emitted photon fluxes are used, each emission spectrum must be corrected and then we must also adjust for the difference in lamp intensity at the two excitation wavelengths using a third spectrum (the excitation spectrum of sodium salicylate). These factors introduce additional error into this measurement. In fact, we evaluated the measurement both ways and found our calculations for the two approaches to agree within a few percent. On the basis of the simplicity of the method,

(8) Abrams, B. L.; Holloway, P. H. *Chem. Rev.* **2004**, *104*, 5783.
(9) Lempicki, A.; Wojtowicz, A. J.; Berman, E. *Nucl. Instrum. Methods Phys. Res., Sect. A* **1993**, *333*, 304.

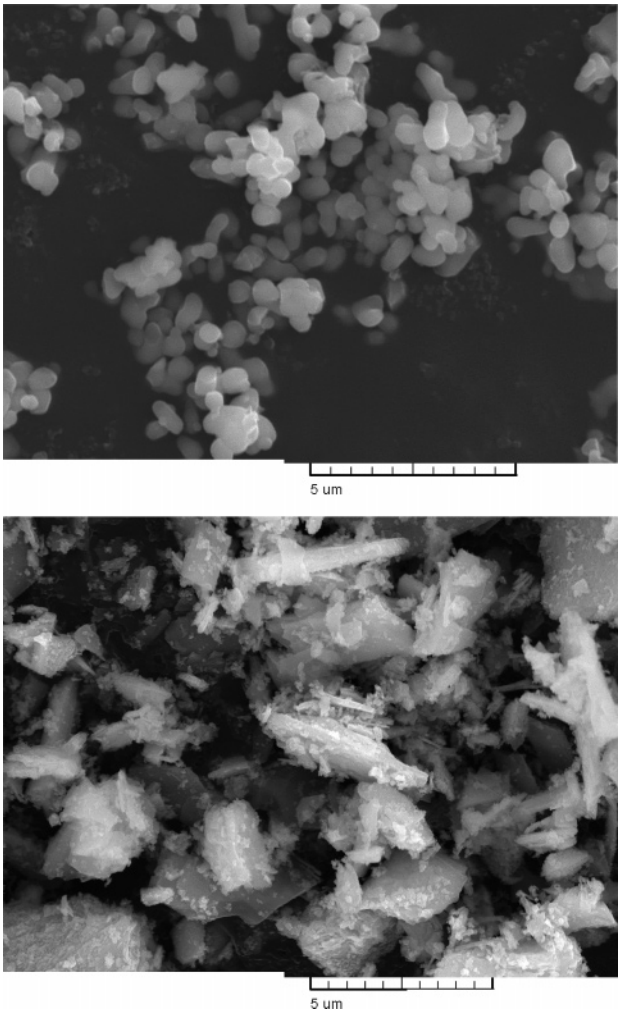

Figure 2. SEM images of YBO_3:Eu (top) and Y_2O_3:Eu (bottom) used in this study.

as well as on the quality of the resulting data, we believe that the excitation spectra provide a very good estimate of the relative emitted photon fluxes under UV and VUV excitation. We also point out that subtle spectral changes in the emission spectra (for example, changes in the relative intensities of various f−f transitions) are not a function of excitation energy and so do not affect the ratios we observe in the excitation spectra.

An important consideration in evaluating the interaction of light with these phosphor powders is their particle size and morphology. Representative scanning electron microscope images are shown in Figure 2 for both materials. The YBO_3:Eu particles are about 1−2 μm and do not have distinct crystal facets. The Y_2O_3:Eu particles are somewhat larger (~5 μm) with much sharper edges in the crystal morphology. The YBO_3 also appears to exhibit a more uniform particle size. While we cannot say how or if these differences may specifically affect the energy transfer properties of these hosts, it is important to note that their light scattering properties appear to be quite similar, as evidenced by the fact that the baseline reflectance relative to MgF_2 is the same for each material. The MgF_2 used in this study has a particle size of approximately 2 μm. We also found no difference in particle size or morphology as a function of europium concentration.

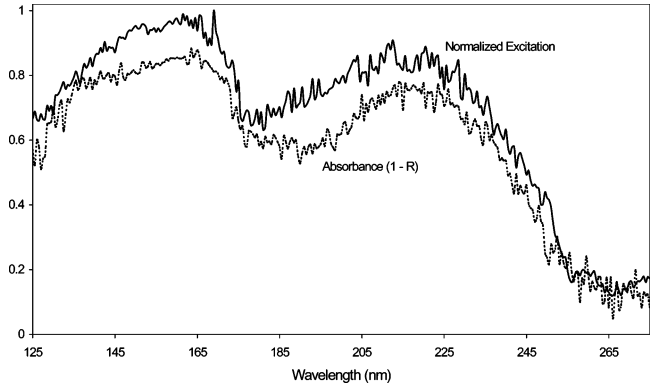

Figure 3. Normalized excitation and absorbance spectra of $Y_{0.90}BO_3:Eu_{0.10}$. Absorbance data are calculated from diffuse reflectance spectra as 1-R.

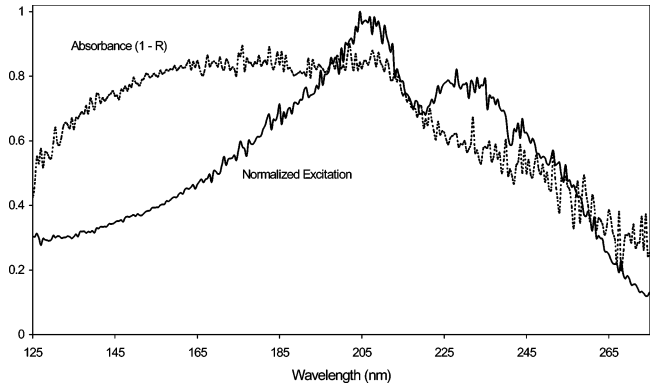

Figure 4. Normalized excitation and absorbance spectra of $Y_{1.90}O_3:Eu_{0.10}$. Absorbance data are calculated from diffuse reflectance spectra as 1-R.

The transfer efficiency will not be identical for all VUV wavelengths. Beyond surface effects, details of the band structure of a given host will be such that excitation at different wavelengths will cause excitation into different electronic states of the lattice. Observed differences between absorption and excitation spectra for a given material are indicative of these differences in the efficiency of energy transfer. To illustrate this point, absorption (as 1-R) and normalized excitation spectra are shown in Figure 3 for $Y_{0.90}BO_3:Eu_{0.10}$ and in Figure 4 for $Y_{1.90}O_3:Eu_{0.10}$. From reflectance spectra on the undoped compounds, we find that the band edge of Y_2O_3 is at 205 nm (5.9 eV) while the band edge of YBO_3 is at 163 nm (7.4 eV). These values are in good agreement with previous reports.[2,5,10] We observe no host lattice emission from the undoped compounds, indicating that host-to-activator energy transfer in these materials is primarily nonradiative.

Direct excitation of Eu^{3+} in these hosts is achieved via an $O-Eu^{3+}$ charge-transfer transition, which we observe as a broad peak at about 232 nm in Y_2O_3 and 220 nm in YBO_3. Both materials exhibit efficient and relatively flat host lattice absorption beyond the band edge. These spectra are consistent with those published by Jüstel et al.[11] The excitation spectrum of $Y_2O_3:Eu^{3+}$ clearly indicates that much of the absorbed energy is not transferred to the activator, particularly at wavelengths shorter than about 185 nm. Figures 3

(10) Mayolet, A.; Krupa, J. C. *Journal for the Society of Information Display* **1996**, *4*, 173.
(11) Jüstel, T.; Krupa, J. C.; Wiechert, D. U. *J. Lumin.* **2001**, *93*, 179.

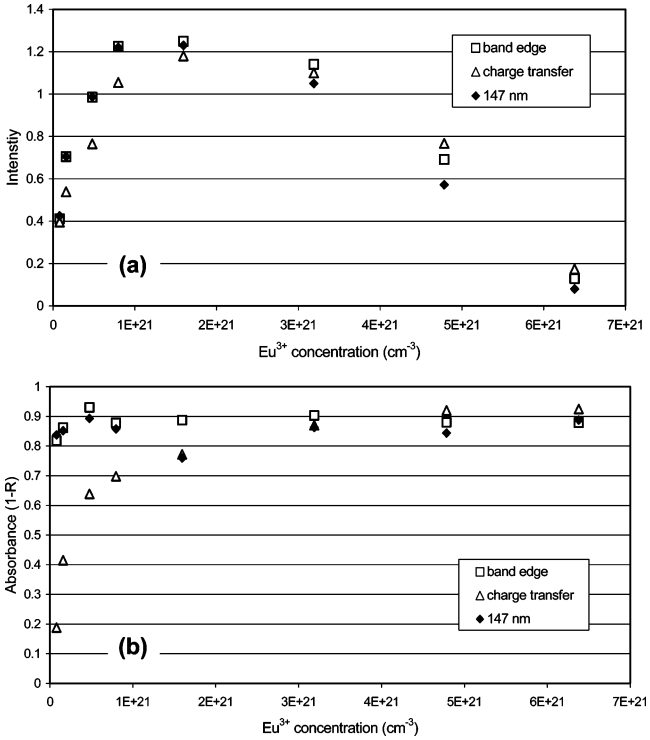

Figure 5. (a) Emission intensity and (b) absorbance data for Eu^{3+}-doped YBO_3. Emission intensities are from excitation spectra of the $^5D_0 \rightarrow {}^7F_2$ transition relative to sodium salicylate. These are the data used for the calculation of η_t in Figure 7.

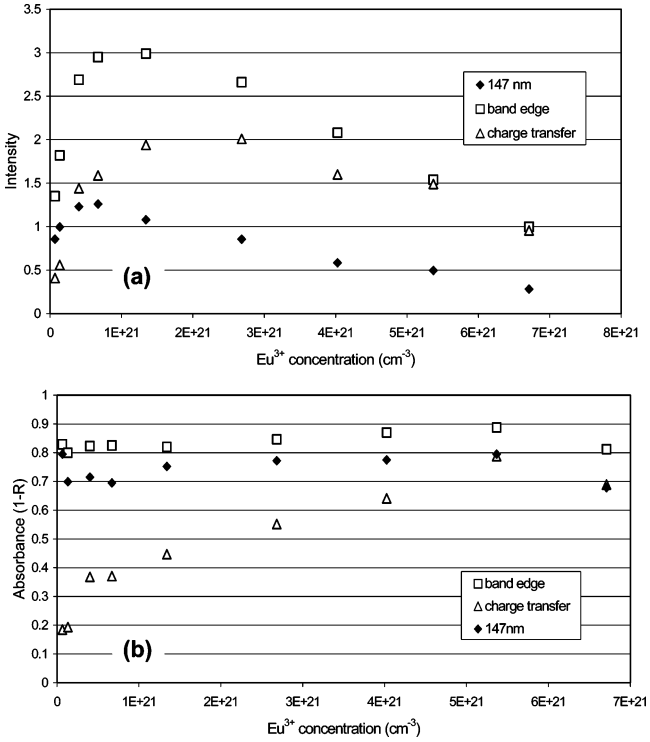

Figure 6. (a) Emission intensity and (b) absorbance data for Eu^{3+}-doped Y_2O_3. Emission intensities are from excitation spectra of the $^5D_0 \rightarrow {}^7F_2$ transition relative to sodium salicylate. These are the data used for the calculation of η_t in Figure 7.

and 4 therefore imply that YBO_3 exhibits a greater transfer efficiency than Y_2O_3 under 147 nm excitation.

To calculate η_t, absorbance and excitation data were collected for a variety of Eu concentrations in each compound. These data are summarized in Figures 5 and 6. Eu concentrations in YBO_3 are calculated on the basis of the orthorhombic cell determined by Morgan et al.[12] and refined by Mishra et al.[13] Although there is some debate in the literature about the exact symmetry of this material, the choice does not affect the number density of Eu. For Y_2O_3 we used the structural data of Paton and Maslen.[14] In Y_2O_3 we also find that the peak of the charge transfer band shifts very slightly to shorter wavelengths as the Eu concentration increases. Maximum intensities were collected at this peak. For each material, the absorbance of the host lattice is independent of activator concentration, while absorption into the charge-transfer band increases with increasing Eu loading, as expected. The data show a peak in the emission intensity at 1.6×10^{21} Eu/cm^3 (10 atom %) in YBO_3, which appears to be independent of the excitation wavelength. Interestingly, in Y_2O_3 the peak in the concentration quenching curve occurs around 2.0×10^{21} (15 atom %) for charge-transfer excitation, at 1.3×10^{21} (10 atom %) for excitation at the band edge, and at 6.7×10^{20} (5 atom %) for excitation at 147 nm. The energy dependence suggests that there may be some interaction between Eu concentration and the degree of surface loss in this host. This conclusion is also supported by the transfer efficiency data reported below.

Calculated energy transfer efficiencies as a function of Eu^{3+} concentration are shown for both compounds in Figure 7, for excitation near the band edge and at 147 nm. In what follows, the assumption is made that the killer concentration does not change with increasing activator concentrations in YBO_3:Eu^{3+} and Y_2O_3:Eu^{3+}. This seems reasonable given that Eu^{3+} and Y^{3+} carry the same charge and have similar ionic radii. Thus we have assumed that the killer concentration is the same within a sample set prepared under identical conditions. In YBO_3:Eu^{3+} the value of η_t increases rapidly with Eu^{3+} concentration and reaches a maximum value of 0.95 by 7.97×10^{20} Eu/cm^3 (5 atom % Eu). At still higher concentrations (>30 atom %) the transfer efficiency decreases again, with the decrease being more dramatic under 147 nm excitation. Note that from a comparison of Figures 5a and 7a, η_t reaches a maximum after concentration quenching has already set in. At high Eu^{3+} concentrations it appears that something has happened to the electronic structure of this phosphor that is promoting greater surface losses, particularly given that the magnitude of the loss increases as the energy of excitation is increased. However, we also cannot rule out the possibility that high Eu loadings influence the defect/bulk killer properties of this host.

For excitation at the band edge in Y_2O_3:Eu^{3+} η_t is fairly high even at low concentrations and reaches a maximum value of about 0.90. The transfer efficiency remains high even at concentrations where significant concentration quenching occurs. At 147 nm, η_t is considerably lower, implying considerable energy loss to surface states. An unusual aspect of these data is the observation that under

(12) Morgan, P. E. D.; Carroll, P. J.; Lange, F. F. *Mater. Res. Bull.* **1977**, *12*, 251.
(13) Mishra, K. C.; DeBoer, B. G.; Schmidt, P. C.; Osterloh, I.; Stephan, M.; Eyert, V.; Johnson, K. H. *Ber. Bunsen-Ges. Phys. Chem.* **1998**, *102*, 1772.
(14) Paton, M. G.; Maslen, E. N. *Acta Crystallogr.* **1965**, *19*, 307.

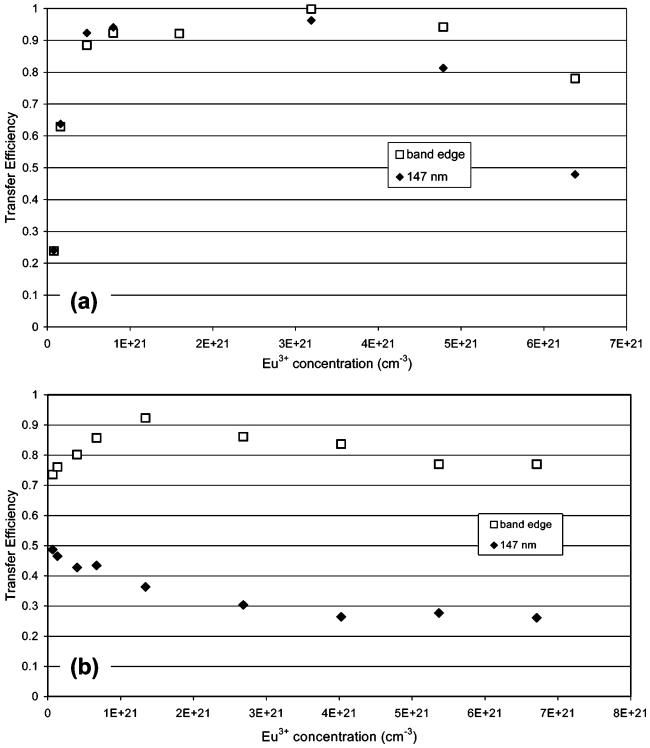

Figure 7. Transfer efficiency, η_t, at room temperature as a function of $[Eu^{3+}]$ for (a) YBO_3 and (b) Y_2O_3. Data are presented for excitation near the band edge and at 147 nm.

147 nm excitation η_t actually decreases slightly with [Eu] before reaching a constant value of about 0.26. This is consistent with the fact that the maximum in the concentration quenching curves shifts to lower concentrations with increasing excitation energy in this phosphor. It appears that the addition of Eu has some influence over the electron transport properties in this material, although VUV concentration quenching at higher Eu appears to be due solely to the well-known higher order effects related to the activator.[3] In YBO_3 these effects are combined with an additional loss of transfer efficiency at high Eu.

Given that interactions of e−h pairs with surface states is a critical component of the models presented here, it is important to know if the surface composition of these phosphors is different from that of the bulk. Depth profiles for both hosts doped at 10% Eu are shown in Figure 8. The data show essentially no variation in composition with depth for Y_2O_3:Eu. This means that the concentration quenching behavior observed in Figure 6a is not due to an enrichment of Eu at the particle surface. In YBO_3, there is a small amount of additional B on the surface, which is presumably due to a borate glass phase. This phase appears to be about 15 nm thick. To our knowledge, data of this type have not previously been published for these materials, so it is not known if this is typical behavior for YBO_3. However, we do not believe that this thin amorphous layer is playing a significant role in the observations we have made here, given that the penetration depth of radiation into YBO_3 has been calculated to be about 73 nm under 147 nm excitation and 135 nm under 160 nm excitation.[15] We also note that SNMS

(15) Moine, B.; Mugnier, J.; Boyer, D.; Mahiou, R.; Schamm, S.; Zanchi, G. *J. Alloys Compd.* **2001**, *323*−*324*, 816.

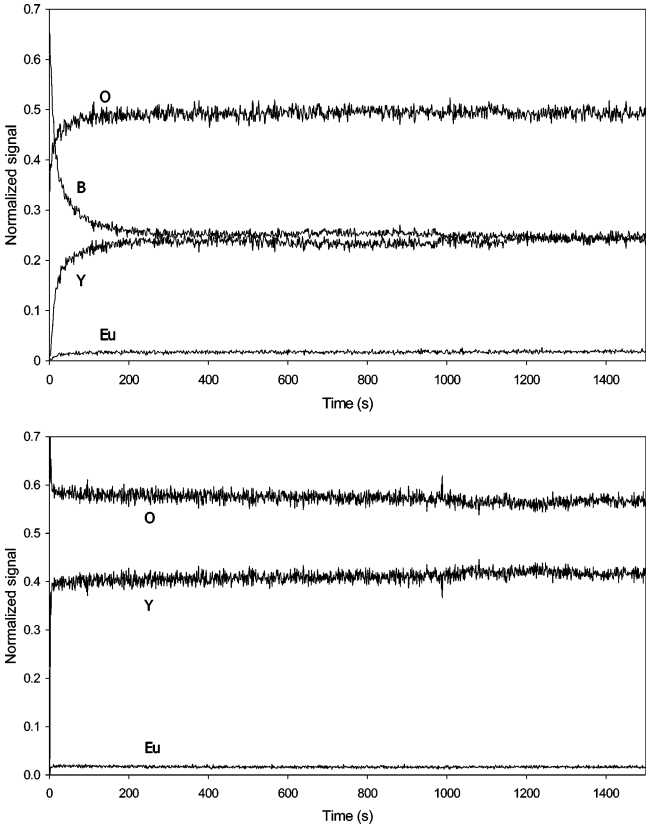

Figure 8. SNMS depth profiles of YBO_3 (top) and Y_2O_3 (bottom) doped at 10 atom % Eu. Sputtering rate is 0.7 Å/s.

measurements on both hosts at 1 and 30 atom % Eu yielded similar results.

Discussion

Precisely modeling the transfer efficiency data (i.e., fitting the data to a calculated curve) is a challenging proposition because of the number of variables involved in the e−h transport and capture process. A complete model would, in particular, require detailed knowledge of how the e−h diffusion length is affected by activator concentration, as well as how the activator influences the surface states of the phosphor. However, in our attempts to apply reasonable fits to these data we have made some general observations that we relate here. The data in Figure 7 are at least qualitatively similar to those shown in Figure 1, and eq 1 can be used to generate estimates of the fit of these data to various α/β ratios. Of course, none of the curves will fit the decrease in η_t we observe at high Eu concentrations because eq 1 does not contain any surface loss terms. In general, any fitting of the band edge excitation data always indicates that Y_2O_3 has a much larger α/β ratio (and therefore relatively greater e−h mobility) than YBO_3. Additionally, in the case of YBO_3 we always find that any fit overestimates the value of η_t for the lowest Eu^{3+} concentrations (0.5 and 1%). Our interpretation of this result is that at low Eu the transfer is e−h diffusion-limited rather than cross-section limited. That is, l_0 in YBO_3 is smaller than the Eu distribution, leading to a low value of the measured η_t. From the Eu concentrations where this deviation takes place, we estimate a value of $l_0 = 15-20$ Å. In Y_2O_3 we do not encounter such a diffusion-limited

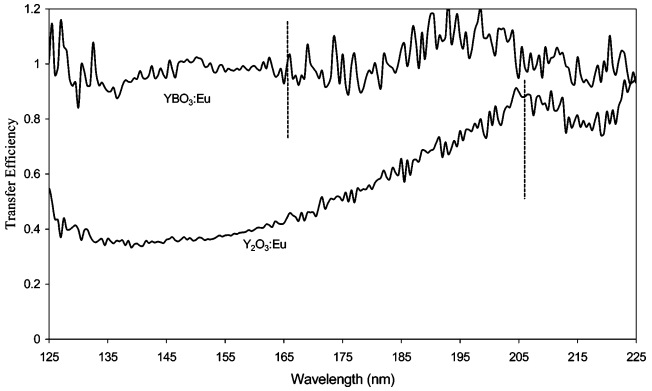

Figure 9. Transfer efficiency, η_t, at room temperature as a function of wavelength in $Y_{0.90}BO_3:Eu_{0.10}$ and $Y_{1.90}O_3:Eu_{0.10}$. Dashed lines indicate the band edge of each host.

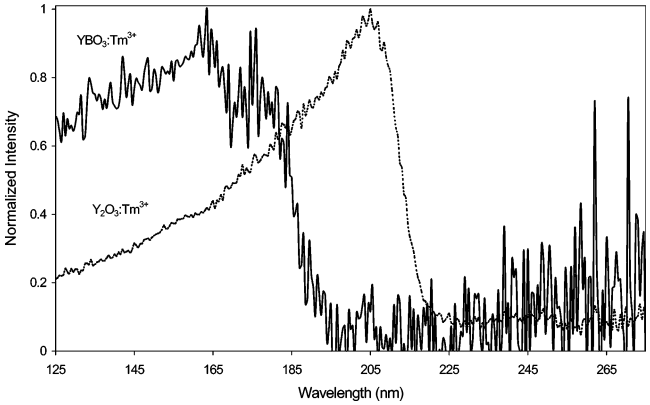

Figure 10. Excitation spectra (λ_{em} = 456 nm) of YBO_3 and Y_2O_3 doped with 10 atom % Tm^{3+}.

regime, which gives a lower limit of about 35 Å for l_0 in that material.

We find that α/β is about 6 times greater in Y_2O_3 than in YBO_3 for excitation near the band edge. That is, for the same Eu concentration e−h migration to activators is actually much more efficient in Y_2O_3 if the excitation energy is just beyond the band gap of the host. However, at 147 nm, the primary operating wavelength of PDPs, energy transfer in Y_2O_3 becomes much less efficient. The significant reduction in transfer efficiency with energy in Y_2O_3 is illustrated in Figure 9, which shows η_t as a function of wavelength for both compounds doped at 10 atom % Eu. The band edge is indicated in these plots, as the calculation of η_t is meaningless at energies lower than the band gap. For YBO_3, η_t is essentially constant down to 125 nm (9.9 eV). In Y_2O_3, η_t decreases continually as the energy of excitation is increased over the range studied. We believe that this is strong evidence for surface loss of excitation energy in this host.

What we have concluded from these experiments is that e−h pairs in Y_2O_3 are much more mobile than they are in YBO_3. Therefore, e−h pairs are more likely to find activators under excitation into the band edge and more likely to find surface states as the excitation energy is increased. In fact, these conclusions are consistent with what has been reported for the electronic structures of both of these hosts.[13] The bottom of the conduction band is dominated by Y 4d states in both materials. However, the conduction band is more disperse in Y_2O_3 and also contains more admixing of O 2p states, which will lead to enhanced electron mobility. Because excitation of Eu^{3+} from the host primarily involves electron trapping,[2] the structure of the conduction band should be the most critical in influencing transfer events. Mishra et al. have also noted that the significant curvature of the conduction band near the Γ point in the band structure of Y_2O_3 may lead to enhanced electron mobility in this material.[16]

To help confirm that the phenomena we observe stem from host rather than from the activator properties, we attempted a similar set of measurements on Tm^{3+}-doped Y_2O_3 and YBO_3. However, the activator quantum efficiency of these materials is very low: no efficient charge transfer excitation and only very weak f−f excitation are observed. Thus, we were unable to perform a complete and detailed analysis in this case. Even so, the spectra obtained do help to confirm the models presented here. VUV excitation data for these hosts doped at 10 atom % Tm are shown in Figure 10. Note the striking similarity of these spectra to those shown in Figures 3 and 4 for the Eu-doped hosts. Although the overall efficiencies are low, it is clear that the transfer efficiency in Y_2O_3 again exhibits a strong energy dependence that is not evident in YBO_3. Reflectance spectra in the host lattice absorption region are the same in these materials regardless of the dopant. In our opinion, these spectra are a good indication that the observations we have made about energy transfer are characteristics of the two hosts.

Conclusion

We have calculated host-to-activator transfer efficiencies in Eu^{3+}-doped YBO_3 and Y_2O_3 as a function of activator concentration, through the measurement of excitation and reflectance spectra. The results indicate that e−h pair mobility is significantly greater in Y_2O_3, while YBO_3 exhibits a relatively shorter diffusion length. Although $Y_2O_3:Eu^{3+}$ is very efficiency under excitation near the band edge, the low brightness of this phosphor under 147 nm excitation is due to a loss of energy to surface states, rather than resulting from inefficient absorption or loss to bulk killers. Spectra of Tm^{3+}-doped compounds show similar properties and indicate that the e−h migration properties we observe are features of the hosts rather than of the activator. These data represent the first quantitative assessment of the energy transfer properties of these hosts under VUV excitation.

Acknowledgment. The authors acknowledge Research Corporation Cottrell College Science Awards and the Faculty Research Fund of Central Washington University for funding support for this work. We also thank Dr. Kailash Mishra for helpful discussions and Erin Macris for assistance with obtaining scanning electron microscopy images.

CM060383L

(16) Mishra, K. C.; Berkowitz, J. K.; Johnson, K. H.; Schmidt, P. C. *Phys. Rev. B* **1992**, *45*, 10902.